Procedia Computer Science

Volume 51, 2015, Pages 286–295

ICCS 2015 International Conference On Computational Science

Dynamics with Matrices Possessing Kronecker Product Structure

M. Łoś[1], M. Woźniak[1], M. Paszyński[1], L. Dalcin[2], and V.M. Calo[2]

[1] AGH University of Science and Technology, Krakow, Poland
[2] King Abdullah University of Science and Technology, Thuwal, Saudi Arabia

Abstract

In this paper we present an application of Alternating Direction Implicit (ADI) algorithm for solution of non-stationary PDE-s using isogeometric finite element method. We show that ADI algorithm has a linear computational cost at every time step. We illustrate this approach by solving two example non-stationary three-dimensional problems using explicit Euler and Newmark time-stepping scheme: heat equation and linear elasticity equations for a cube. The stability of the simulation is controlled by monitoring the energy of the solution.

Keywords: isogeometric finite element method, non-stationary problems, alternating direction solver, linear computational cost

1 Introduction

The Alternating Direction Implicit (ADI) algorithm has been originally introduced in [1, 2, 3, 4] to solve parabolic problems. The method has been applied to two-dimensional non-stationary problems [6], and also as a preconditioner for iterative solvers in case of complex geometries [7]. In this paper we focus on the application of the ADI algorithm to three-dimensional non-stationary parabolic problems and their non-linear extensions solved with the ADI algorithm using isogeometric analysis [5]. We test our isogeometric $3D$ ADI algorithm on two different computational problems: $3D$ model heat transfer problem and $3D$ linear elasticity problem. For the first problem we employ the Euler scheme, for the second one the Newmark time integration scheme. We show that our ADI solver has a linear computational cost at every time step.

2 Algorithm

The algorithm solves unsteady partial differential equations with FEM using explicit Euler scheme and the ADI solver. The time-stepping scheme is standard and shown in Algorithm 1.

The ADI solver is detailed in [8, 6]. We briefly summarize the main ideas below. A Second-order non-stationary parabolic differential equation discretized with the forward Euler scheme

 Selection and peer-review under responsibility of the Scientific Programme Committee of ICCS 2015

doi:10.1016/j.procs.2015.05.243

$u^{(0)} \leftarrow$ projection of initial state $u(x,0)$;
for $t \in \{0,\ldots,T-1\}$ **do**
  $\mathbf{S} \leftarrow L^2$-projection of RHS of equation 1, computed using $u^{(t)}$;
  compute $u^{(t+1)}$ from $\mathbf{M}\,u^{(t+1)} = \mathbf{S}$ using Alternating Direction Solver
end

Algorithm 1: Nonstationary-Forward-Euler

in time and the Galerkin method in space results in the following matrix equation:

$$\mathbf{M}\,u^{(t+1)} = \mathbf{M}\,u^{(t)} + \Delta t\left(\mathbf{S}\,u^{(t)} + \mathbf{F}\right) \tag{1}$$

Using isogeometric FEM with tensor product basis, under certain assumptions, matrix $\mathbf{M}$ can be decomposed as a tensor (Kronecker) product of three matrices corresponding to dimensions of the domain. Following [6], we call such $\mathbf{M}$ *separable*. Assuming matrix M is separable with Kronecker decomposition $M = M_x \otimes M_y \otimes M_z$, we can exploit this structure and commutativity of tensor product and inversion:

$$(A \otimes B)^{-1} = A^{-1} \otimes B^{-1} \tag{2}$$

to solve system of equations given by $Mu = b$ by solving multiple systems of equations separately in each direction, as specified in Algorithm 2.

Input: $M = M_x \otimes M_y \otimes M_z$ - matrix, u - unknown, b - RHS
Result: Solution of $Mu = b$
$u'(\cdot,j,k) = M_x^{-1} b(\cdot,j,k)$;
$u''(i,\cdot,k) = M_y^{-1} u'(i,\cdot,k)$;
$u(i,j,\cdot) = M_z^{-1} u''(i,j,\cdot)$;

Algorithm 2: Alternating Direction Solver

Matrices M_x, M_y and M_z are banded with bandwidth $2p+1$, where p is the degree of used B-spline basis. Assuming we use basis that is a tensor product of one-dimensional bases with N_x, N_y and N_z degrees of freedom, respectively, applying the inverse of M using the above algorithm is equivalent to applying inverses of M_x to N_yN_z vectors, M_y to N_xN_z vectors and M_z to N_xN_y vectors. As applying the inverse of M_x can be done in $O(N_x)$ thanks to its banded structure, this stage has complexity $O(N_xN_yN_z)$, and similarly for M_y and M_z. Thus, the whole process can be performed in $O(N_xN_yN_z)$, i.e. in time linear with respect to number of degrees of freedom $N = N_xN_yN_z$.

3 Example problems

In all the following problems, open-knot B-splines of degree 2 (locally quadratic) were used as basis functions.

3.1 Heat equation

The first solved problem is the classical heat transport equation, given by

$$\begin{cases} \dfrac{\partial u}{\partial t} = \Delta u & \text{on } \Omega \times [0,T] \\ \nabla u \cdot \hat{n} = 0 & \text{on } \partial\,\Omega \times [0,T] \\ u(x,0) = u_0 & \text{on } \Omega \end{cases} \tag{3}$$

where $\Omega = [0,1]^3$, and the initial state is a ball of heat centered at $(0.5, 0.5, 0.5)$ with diameter 0.5, as displayed in figure 1. First, we show that solution of 3 is unique.

Lemma 1. *Let u be solution of equation 3, and*

$$e_u(t) = \int_\Omega u^2(x,t)\,\mathrm{d}\Omega$$

Then e_u is non-increasing function of t.

Proof. We have

$$\frac{\partial}{\partial t} e_u = \int_\Omega \frac{\partial u^2}{\partial t}\,\mathrm{d}\Omega = 2\int_\Omega u \frac{\partial u}{\partial t}\,\mathrm{d}\Omega = 2\int_\Omega u \Delta u\,\mathrm{d}\Omega$$

By Green's first identity and the Neumann boundary conditions,

$$\int_\Omega u\Delta u + \|\nabla u\|^2\,\mathrm{d}\Omega = \int_\Gamma u\,\nabla u \cdot \hat{n}\,\mathrm{d}\Gamma = 0$$

therefore

$$\frac{\partial}{\partial t} e_u = -2\int_\Omega \|\nabla u\|^2\,\mathrm{d}\Omega \le 0$$

□

Theorem 1. *If equation 3 possesses a solution, it is unique.*

Proof. Let u, v be solutions to equation 3. Due to linearity, $u - v$ is a solution to equation 3 with $u_0 = 0$, hence applying the lemma to $u - v$ shows that e_{u-v} is non-increasing. But $e_{u-v}(0) = 0$, hence $e_{u-v} = 0$ (since it is non-negative by definition), and therefore $u = v$. □

The weak form of equation 3 is obtained by multiplying by $w \in H^1(\Omega)$ both sides and integrating over Ω, and discretized with forward Euler scheme, yielding

$$\langle u^{(t+1)}, w\rangle = \langle u^{(t)}, w\rangle + \Delta t \langle \Delta u, w\rangle \tag{4}$$

Using Green's first identity for the part with the Laplacian and utilizing zero Neumann boundary condition gives

$$\langle u^{(t+1)}, w\rangle = \langle u^{(t)}, w\rangle - \Delta t \int_\Omega \langle \nabla u, \nabla w\rangle\,\mathrm{d}\Omega \tag{5}$$

for all $w \in H^1(\Omega)$.

The time step used for the simulation was $\Delta t = 10^{-4}$. It was chosen empirically to ensure stability of the computation, using CFL condition as a starting point. Results (cross-sections through a plane $z = 0.5$) are depicted in figure 1.

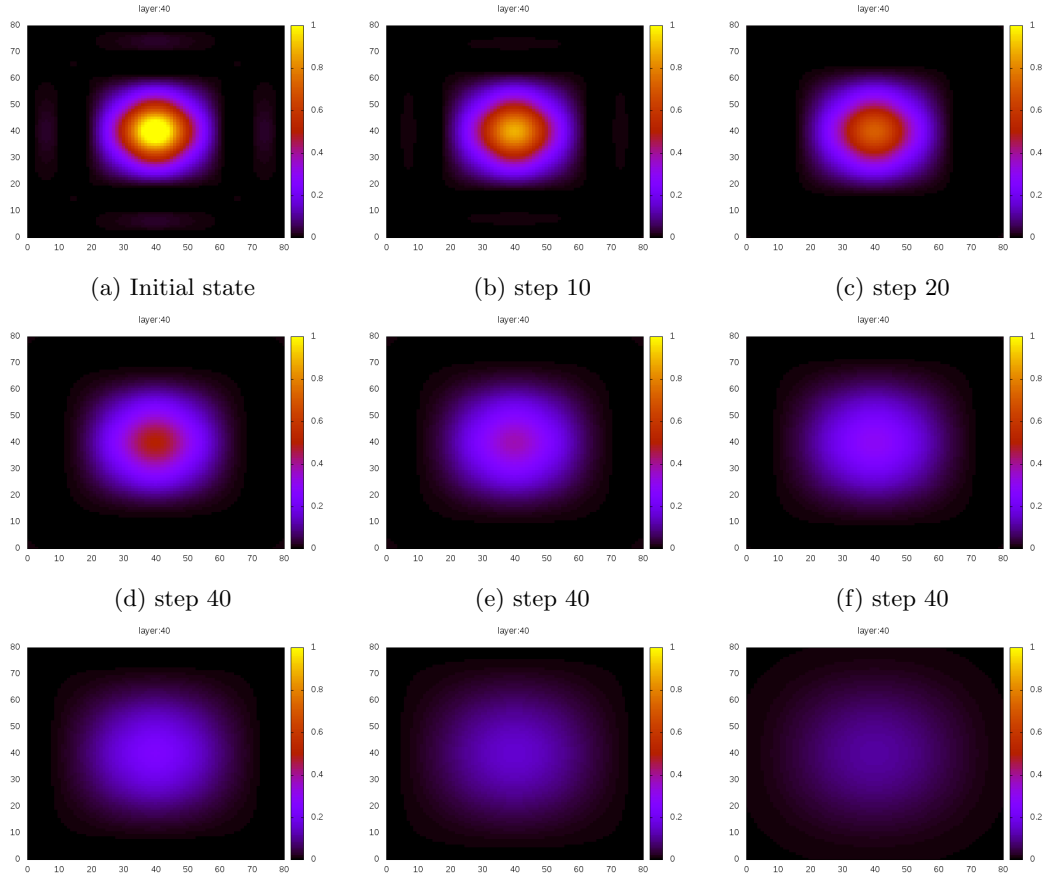

(a) Initial state (b) step 10 (c) step 20

(d) step 40 (e) step 40 (f) step 40

(g) step 40 (h) step 100 (i) step 200

Figure 1: Solution of the heat transport equation

3.2 Linear elasticity

The second problem is the small strain linear elasticity equation, describing deformation of solid objects in presence of an external force. Strong form of the equation is given by

$$\begin{cases} \rho \dfrac{\partial^2 \mathbf{u}}{\partial t^2} = \nabla \cdot \boldsymbol{\sigma} + \mathbf{F} & \text{on } \Omega \times [0,T] \\ \boldsymbol{u}(x,0) = u_0 & \text{for } x \in \Omega \\ \boldsymbol{\sigma} \cdot \hat{\mathbf{n}} = 0 & \text{on } \partial\,\Omega \end{cases} \tag{6}$$

where $\Omega = [0,1]^3$ is an unit cube, $\mathbf{u}$ is a 3-dimensional displacement vector to be calculated, ρ is material density, $\mathbf{f}$ is the applied external force, and $\boldsymbol{\sigma}$ is rank-2 stress tensor, given by

$$\sigma_{ij} = c_{ijkl}\epsilon_{lk} \tag{7}$$

where

$$\epsilon_{ij} = \frac{1}{2}\left(\partial_j u_i + \partial_i u_j\right) \tag{8}$$

and $\mathbf{c}$ is a rank-4 elasticity tensor (Einstein summation convention applies in the proceeding equation). For our simulations we assumed isotropic material with Lamé coefficients $\lambda = \mu = 1$.

In order to utilize forward Euler integration scheme, the above system of 3 equations is converted to system of 6 equations by introducing additional variables corresponding to components of displacement's velocity:

$$\mathbf{v_i} = \frac{\partial \mathbf{u_i}}{\partial t} \tag{9}$$

Corresponding weak formulation discretized with the explicit Newmark's scheme (with $\beta = \gamma = 0$) is given by

$$\begin{cases} \langle u_i^{(t+1)}, w\rangle = \langle u_i^{(t)} + \Delta t\, v_i^{(t)} + \dfrac{\Delta t^2}{2} a_i^{(t)}, w\rangle \\ \langle v_i^{(t+1)}, w\rangle = \langle v_i^{(t)} + \Delta t\, a_i^{(t)}, w\rangle \\ a_i^{(t)} = \dfrac{1}{\rho}\left(\sigma_{ij,j} + F_i\right) \end{cases} \tag{10}$$

for all $w \in H^1(\Omega)$, where $\langle \cdot, \cdot \rangle$ denotes standard scalar product in $L^2(\Omega)$, and $u_i, v_i \in H^1(\Omega)$.

The energy of the system consists of two parts: kinetic energy, due to change of displacement, and potential energy, due to material's resistance to distortions. These energies are given by

$$\begin{aligned} E_k &= \frac{1}{2}\int_\Omega \rho \left\|\mathbf{v}\right\|^2 \mathrm{d}\Omega \\ E_p &= \frac{1}{2} c_{ijkl}\epsilon_{ij}\epsilon_{kl} = \frac{1}{2}\boldsymbol{\sigma} : \epsilon \end{aligned} \tag{11}$$

3.2.1 Initial deformation, no force

In the first tested variant, no external force is applied ($\mathbf{F} = 0$) and the cube is initially sheared along an x axis, that is

$$u_0(x) = (10^{-3}z, 0, 0) \tag{12}$$

Solution of the problem is depicted in figure 2. Deformation is magnified 200 times to make it visible.

With no force present, total energy of the system should remain constant. This is, however, not the case in our simulation. Figure 3 displays total energy growth for various mesh sizes and degrees of B-splines used. The growth increases with number of floating-point operations, which suggests it occurs due to round-off errors. Due to long duration of the full simulation, these tests were limited to 2,300 iterations. There was no such issue with heat and flow equations (without forcing) – in these problems, the energy was approximately constant throughtout the simulation, as expected. We have also performed the simulation with Lamé coefficients $\lambda = 0, \mu = 1$, which corresponds to zero Poisson ratio, and we have obtained indentical numerical behaviour of the method. This is expected, since algebraically we solve identical problem, as the $3D$ problem, so there is no decoupling there. This confirms our hipothesis that the growth of energy is related to round-off error.

17,000 iterations have been performed on a machine with Intel Core i5-2410M CPU (4 cores, 2.3 GHz) and 4 GB of RAM. Total time of the main simulation was 24,790 seconds (almost 7 hours). Times of the short simulations whose results are displayed in figure 3, were linear with respect to number of degrees of freedom, as expected.

Note that our algorithm performs 17,000 iterations, and the average execution time per iteration is around 1.5 seconds. Thus, the long execution time is due to the large number of iterations performed.

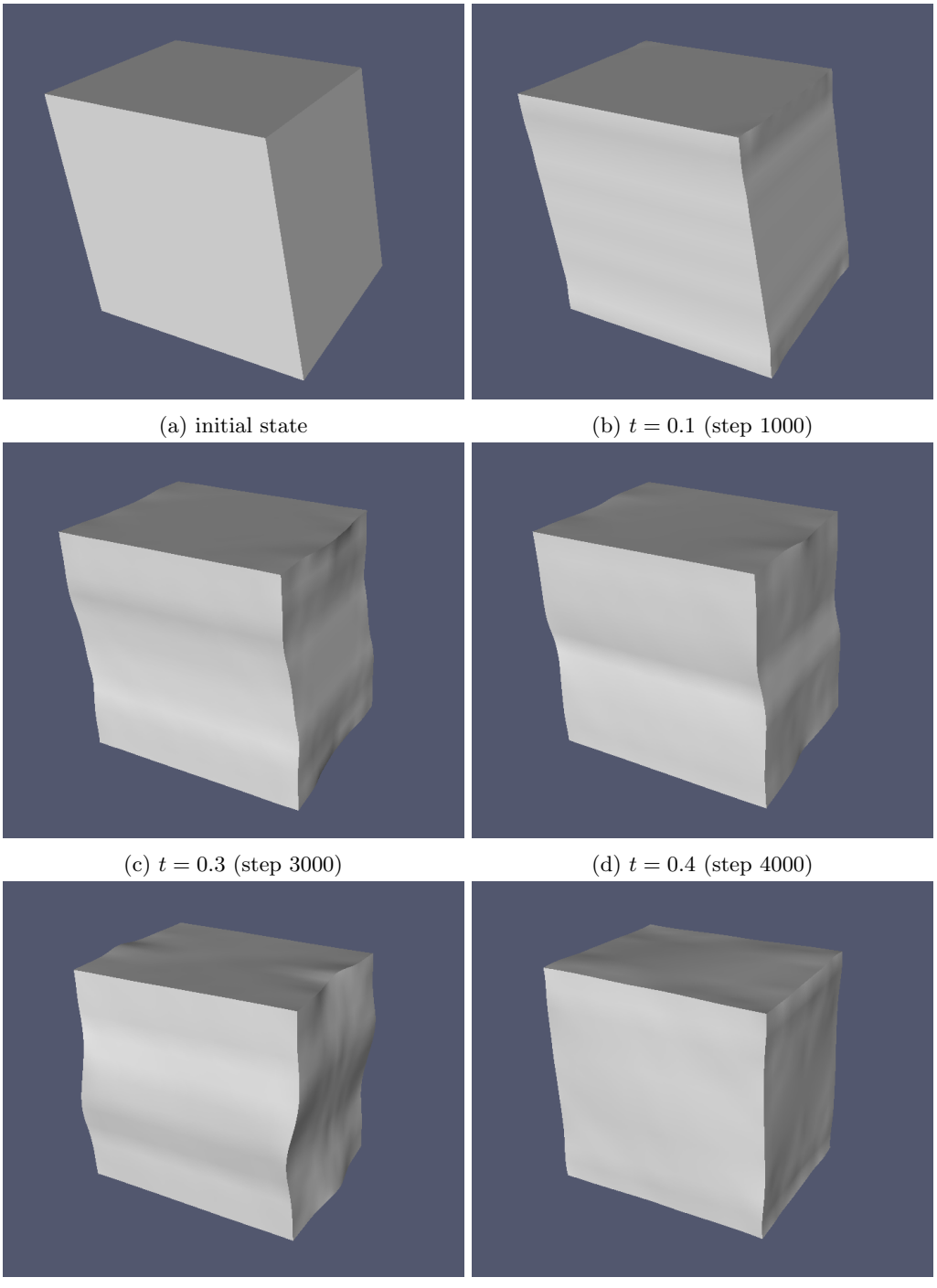

(a) initial state

(b) $t = 0.1$ (step 1000)

(c) $t = 0.3$ (step 3000)

(d) $t = 0.4$ (step 4000)

(e) $t = 0.7$ (step 7000)

(f) $t = 1$ (step 10000)

Figure 2: Deformation of cube – initial shear

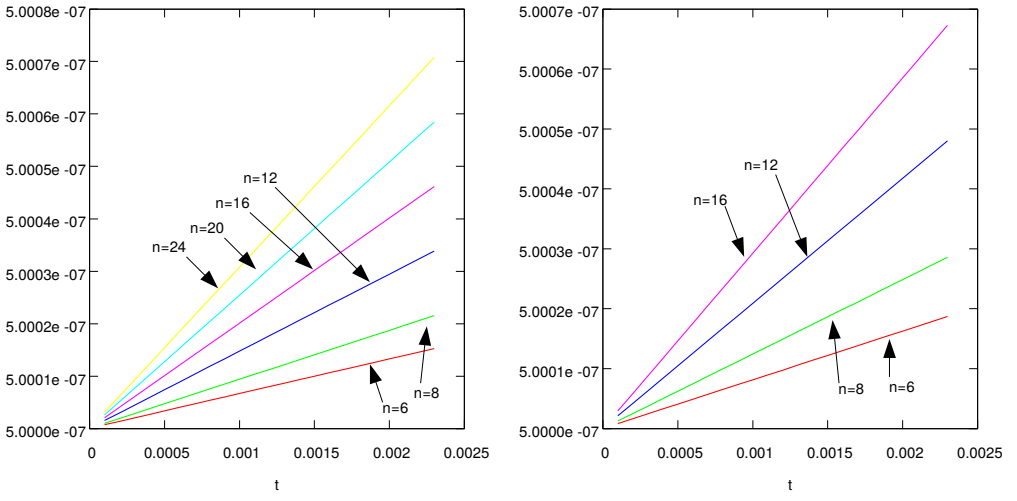

(a) $p = 2$ (b) $p = 3$

Figure 3: Deformed cube – energy of the solution (n – number of degrees of freedom)

3.2.2 No initial deformation, applied force

In the second tested variant, cube is initially not deformed, but a non-zero force is applied. The force is given by

$$\mathbf{F}(\mathbf{x}, t) = -\phi(t/t_0) r(\mathbf{x})\, \mathbf{p} \tag{13}$$

$$\mathbf{p} = (1, 1, 1) \tag{14}$$

$$t_0 = 0.02 \tag{15}$$

$$\phi(t) = \begin{cases} t^2(1-t)^2 & \text{if } t \in (0,1) \\ 0 & \text{otherwise} \end{cases} \tag{16}$$

$$r(\mathbf{x}) = 10 \exp\left(-10 \left\|\mathbf{x} - \mathbf{p}\right\|^2\right) \tag{17}$$

i.e. it is a short impulse directed towards the origin, applied at the opposite corner of the cube.

Figure 4 displays results of the simulation with the time step $\Delta t = 10^{-4}$. Displacement is magnified 20 times to make it visible.

Figure 5a shows the energy of the solution as a function of time. Since initially the cube is not deformed and is at rest, it has zero total energy. When the short force impulse is applied, kinetic energy of the system experiences a rapid growth, as the force accelerates the corner of the cube. Due to elastic response to deformation, kinetic energy decreases and the potential energy builds up. Subsequently, as the deformation propagates inside the cube, kinetic and potential energies oscillate (the cube ,,bounces"), but after the impulse total energy of the system should remain constant. As in the previous problem, however, a small (of the order 10^{-6}) but steady growth of total energy is visible on the plot (shown in detail in figure 5b). After 30,000 steps the growth is around 1.6×10^{-6} (1.5% of the total energy).

As in the previous case, we believe the growth to be due to round-off error. Our method seems more sensitive to the round-off error, because we solve three $1D$ problems with multiple right-hand sides. The $1D$ problem is more sensitive to the round-off error than $3D$ problem.

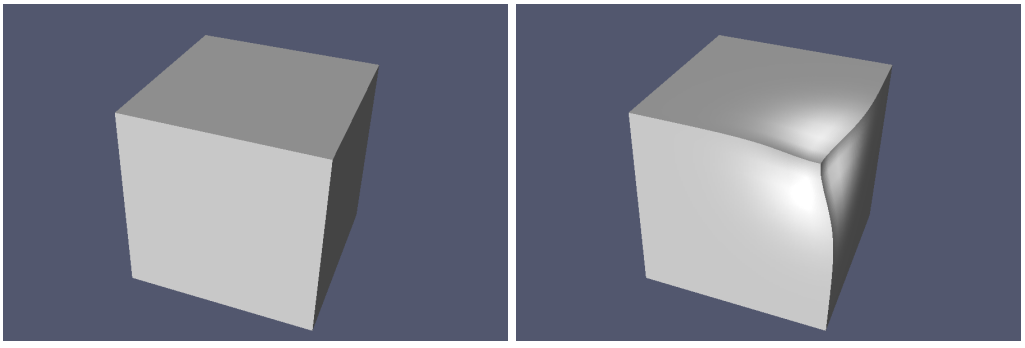

(a) initial state (undeformed)

(b) step 1000

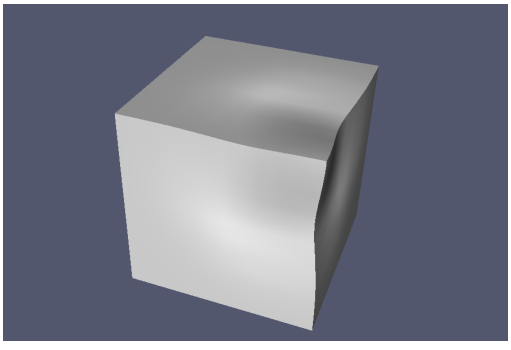

(c) step 4000

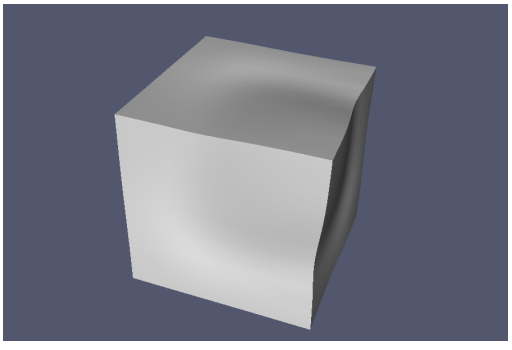

(d) step 6000

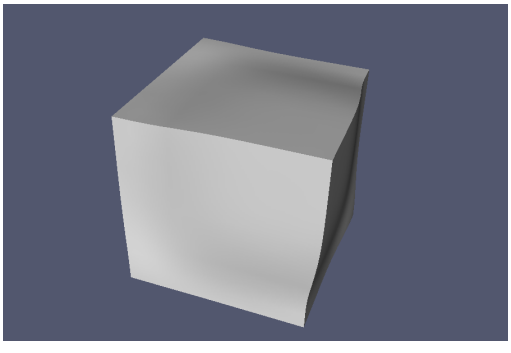

(e) step 8000

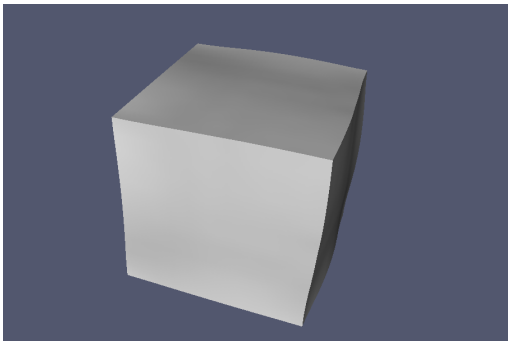

(f) step 10000

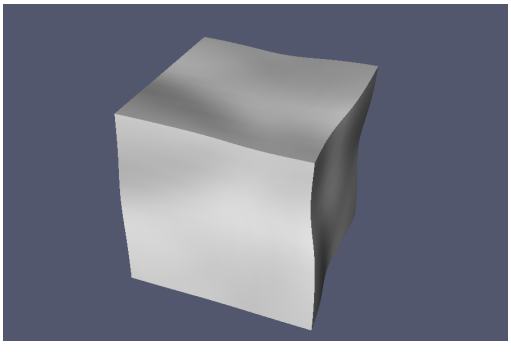

(g) step 14000

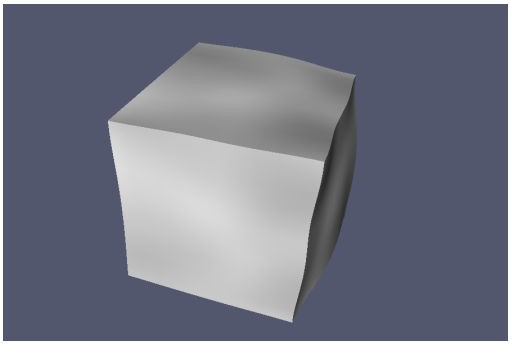

(h) step 18000

Figure 4: Deformation of cube – force applied in the corner

The energy growth has been analyzed for various combinations of mesh sizes and degrees of B-splines. Results are presented in figure 6. The energy grows with size of the mesh, although the relation is less clear than in the variant without the force. Additionally, simulation with force applied at different point and angle has been carried out, and resulted in very similarly shaped energy curves.

30,000 iterations have been performed, total time of the simulation was 39,233 seconds (around 11 hours).

4 Conclusions and future work

In this paper we presented the application of the Alternating Directions Implicit solver to solving three-dimensional non-stationary problems using isogeometric finite element method. We tested the algorithm on model heat transfer problem and on the linear elasticity problem. For the last problem, 30,000 iterations was performed in less than 11 hours (1.46 seconds per iteration on average) on a single machine with Intel Core i5-2410M CPU (4 cores, 2.3 GHz) and 4 GB of RAM. The future work will involve the execution of parallel version of the non-stationary solver.

5 Acknowledgments

The work of ML and MP has been supported by Polish National Science Center grant no. DEC-2012/07/B/ST6/01229 and DEC-2011/03/B/ST6/01393. The work of VMC and LD as well as visits of ML, MP and MW at KAUST has been supported by Center for Numerical Porous Media. The work of MW has been supported by deans grant.

References

[1] D.W. Peaceman, H.H. Rachford Jr., The numerical solution of parabolic and elliptic differential equations, Journal of Society of Industrial and Applied Mathematics 3 (1955) 2841

[2] J. Douglas, H. Rachford, On the numerical solution of heat conduction problems in two and three space variables, Transactions of American Mathematical Society 82 (1956) 421439

[3] E.L. Wachspress, G. Habetler, An alternating-direction-implicit iteration technique, Journal of Society of Industrial and Applied Mathematics 8 (1960) 403423

[4] G. Birkhoff, R.S. Varga, D. Young, Alternating direction implicit methods, Advanced Computing 3 (1962) 189273

[5] J. A. Cottrell, T. J. R. Hughes, Y. Bazilevs, *Isogeometric Analysis: Toward Unification of CAD and FEA* John Wiley and Sons, (2009)

[6] L. Gao, V.M. Calo, Fast Isogeometric Solvers for Explicit Dynamics, Computer Methods in Applied Mechanics and Engineering, 274 (1) (2014) 19-41

[7] L. Gao, V.M. Calo, Preconditioners based on the alternating-direction-implicit algorithm for the 2D steady-state diffusion equation with orthotropic heterogenous coefficients, Journal of Computational and Applied Mathematics, 273 (1) (2015) 274-295

[8] L. Gao, Kronecker Products on Preconditioning, PhD. Thesis, King Abdullah University of Science and Technology (2013)

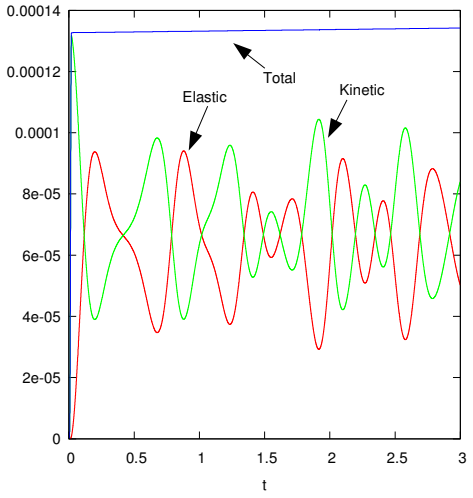

(a) Kinetic, elastic and total energy

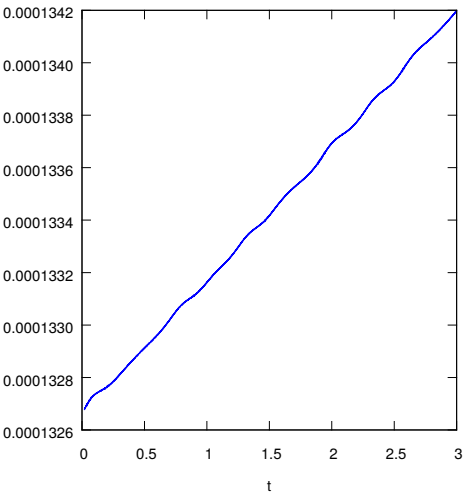

(b) Drift of the total energy – closeup

Figure 5: Energy of the cube as a function of time

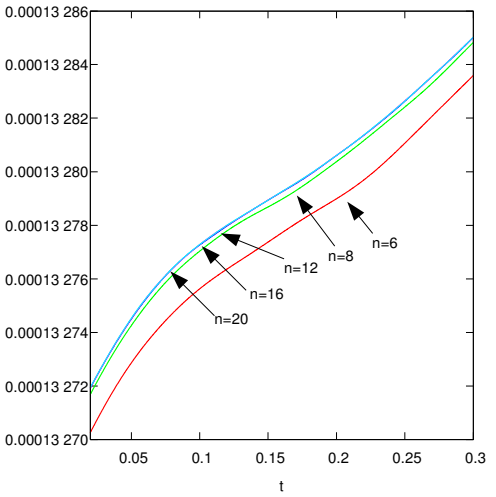

(a) $p = 2$

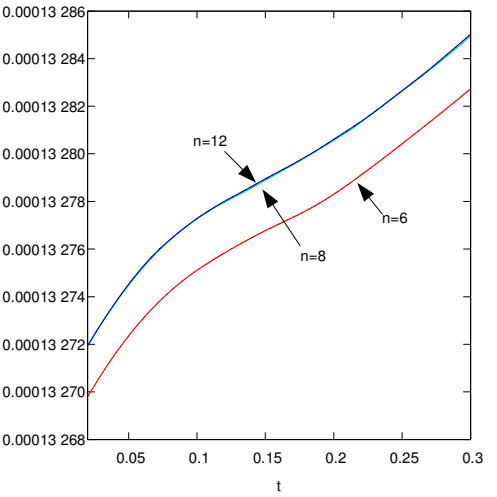

(b) $p = 3$

Figure 6: Growth of the energy after the initial impulse for various mesh sizes